Coherent d-Wave Superconducting Gap in Underdoped $La_{2-x}Sr_xCuO_4$ by Angle-Resolved Photoemission Spectroscopy

M. Shi,[1] J. Chang,[2] S. Pailhés,[2] M. R. Norman,[3] J. C. Campuzano,[4,3] M. Månsson,[5] T. Claesson,[5] O. Tjernberg,[5] A. Bendounan,[2] L. Patthey,[1] N. Momono,[6] M. Oda,[6] M. Ido,[6] C. Mudry,[7] and J. Mesot[2]

[1]*Swiss Light Source, Paul Scherrer Institute, CH-5232 Villigen PSI, Switzerland*
[2]*Laboratory for Neutron Scattering, ETH Zurich and Paul Scherrer Institute, CH-5232 Villigen PSI, Switzerland*
[3]*Materials Science Division, Argonne National Laboratory, Argonne, Illinois 60439, USA*
[4]*Department of Physics, University of Illinois at Chicago, Chicago, Illinois 60607, USA*
[5]*Materials Physics, Royal Institute of Technology KTH, S-164 40 Kista, Sweden*
[6]*Department of Physics, Hokkaido University Sapporo 060-0810, Japan*
[7]*Condensed Matter Theory Group, Paul Scherrer Institute, CH-5232 Villigen PSI, Switzerland*
(Received 15 August 2007; published 24 July 2008)

We present angle-resolved photoemission spectroscopy data on moderately underdoped $La_{1.855}Sr_{0.145}CuO_4$ at temperatures below and above the superconducting transition temperature. Unlike previous studies of this material, we observe sharp spectral peaks along the entire underlying Fermi surface in the superconducting state. These peaks trace out an energy gap that follows a simple d-wave form, with a maximum superconducting gap of 14 meV. Our results are consistent with a single gap picture for the cuprates. Furthermore our data on the even more underdoped sample $La_{1.895}Sr_{0.105}CuO_4$ also show sharp spectral peaks, even at the antinode, with a maximum superconducting gap of 26 meV.

The energy gap is a fundamental property of superconductors [1]. The nature of its anisotropy has played a key role in the testing and building of microscopic theories of the superconductivity discovered in layered copper oxides [2]. This anisotropy can be measured by angle-resolved photoemission spectroscopy (ARPES), which is a unique probe of electronic excitations and their momentum dependence [3,4]. For underdoped samples, an energy gap persists above T_c [5,6]. This pseudogap is most prominent in the $(\pi, 0)$ region of the Brillouin zone, giving rise to a gapless arc of states centered about the zone diagonal known as a Fermi arc [7]. How the gap evolves from the superconducting state to the pseudogap phase remains one of the most important questions being debated in the cuprates [8]. It has been suggested that the superconducting gap only exists on the Fermi arcs, and thus is distinct from the pseudogap [9]. This "two gap" scenario has been supported by recent ARPES studies on optimally doped $La_{2-x}Sr_xCuO_4$ (LSCO) [10] and $Bi_2Sr_2CuO_6$ (Bi2201) [11], as well as on heavily underdoped Bi2212 [12]. In these studies, sharp spectral peaks are observed below T_c only along the arc, whereas the states in the region around the $(\pi, 0) - (\pi, \pi)$, Fermi crossing (the antinode) remain incoherent, as they were above T_c. Moreover, the size of the energy gap in the antinodal region is significantly larger than that expected from a simple extrapolation of the gap from the arc.

Our ARPES results on moderately underdoped LSCO ($x = 0.145$) reveal a very different picture. Similar to previous studies of underdoped Bi2212 [13], below T_c we observe sharp spectral peaks along the entire underlying Fermi surface (FS), which trace out a simple d-wave

gap with a maximum amplitude of 14 meV. For more underdoped LSCO ($x = 0.105$) the spectra are still characterized by coherent peaks in the $(\pi, 0)$ region with a maximal gap amplitude of 26 meV. We see no evidence for a much larger gap in the antinodal region as reported in other studies [10–12]. More significantly, we find that the superconducting and pseudogaps have similar maximum amplitudes.

ARPES results were obtained on very high-quality single crystals of LSCO, grown using the traveling solvent floating zone method [14], with a transition temperature $T_c = 36$ K and 30 K for $x = 0.145$ and $x = 0.105$, respectively. The transition width for both dopings are $\Delta T_c \approx 1.5$ K. ARPES experiments were carried out at the surface and interface spectroscopy beam line at the Swiss Light Source. During the measurements, the base pressure always remained less than 5×10^{-11} mbar. The ARPES spectra were recorded with a Scienta SES2002 electron analyzer with an angular resolution of better than 0.15°. Circularly polarized light with $h\nu = 55$ eV and linearly polarized light with $h\nu = 25$ eV were used. The energy resolutions were 17 and 12 meV for $h\nu = 55$ and 25 eV, respectively. The Fermi level was determined by recording the photoemission spectra from polycrystalline copper on the sample holder. The samples were cleaved *in situ* by using a specially designed cleaving tool [15]. Clear (1×1) low-energy electron-diffraction patterns obtained after the ARPES measurements indicate that the cleaved surfaces had good quality.

Figure 1 shows typical ARPES intensity maps of LSCO ($x = 0.145$) in the superconducting phase as a function of wave vector and energy in the nodal region [Fig. 1(a)], in
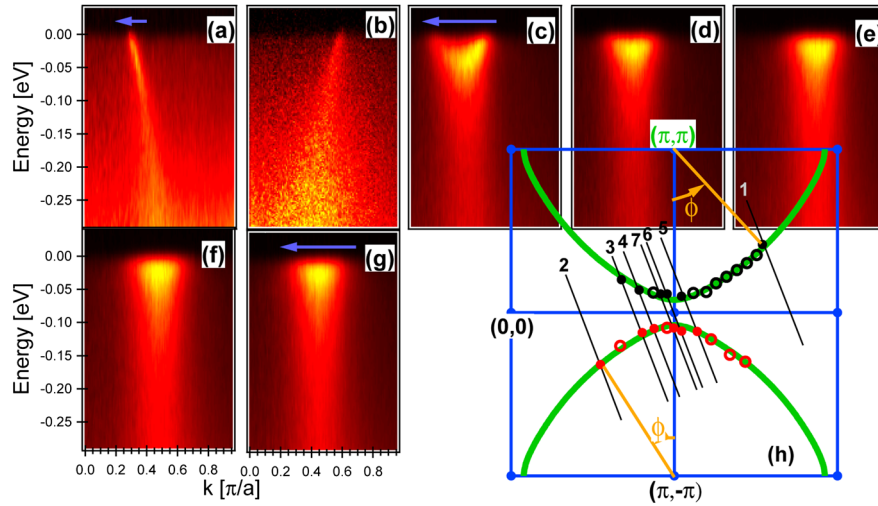
FIG. 1 (color online).   ARPES intensities along momentum cuts that cross the underlying Fermi surface (FS) (a) at the node, (b)–(f) between the node and the antinode, and (g) at the antinode. The corresponding cuts 1–7 are indicated in (h). The circles in (h) are the underlying FS determined from our measurements, while the solid line is the FS from a tight-binding fit to our data. The measurements were performed on LSCO ($T_c = 36$ K, $x = 0.145$) at 12 K with $h_\nu = 55$ eV.

the antinodal region [Figs. 1(f) and 1(g)], and between these two regions [Figs. 1(b)–1(e)]. While the spectral peaks close to the nodal direction exhibit a sizable dispersion, the dispersion is much weaker in the antinodal region, which is the ubiquitous behavior among hole-doped cuprates in the superconducting state. We used two different methods to determine the underlying normal state FS. In the first case, it was obtained from the peak positions of the momentum distribution curves at zero binding energy along momentum cuts parallel to those shown in Fig. 1(h), and in the second method, it was identified by searching for the minimum gap location of the energy distribution curves (EDCs) along each cut. Both methods gave the same result. From a tight-binding fit to the underlying FS, we obtain a hole volume of 57.2%, corresponding to 1.144 holes per Cu atom, in agreement with the Sr doping level of $x = 0.145$.

It is important to mention that we have observed sharp spectral peaks along the *entire* underlying FS in the superconducting state. To visualize this, in Fig. 2 we plot EDCs along the momentum cuts 1, 3, and 7 in Fig. 1(h) in reduced momentum ranges. The corresponding momentum windows are marked in Figs. 1(a), 1(c), and 1(g) with arrows. A comparison of the spectrum at the node and the antinode is given in Fig. 2(d). One can see both spectra are characterized by a sharp peak with a similar width. The true widths of these peaks are even smaller, given the energy resolution (17 meV) used in these measurements. To demonstrate this, based on the observation that the spectral peaks disperse only weakly in the (π, 0) region, we collected an angle-integrated EDC in the momentum window marked in Fig. 1(g) by the arrow with a higher energy resolution of 12 meV. Indeed, as expected, the peak narrows in energy as can be seen in Fig. 2(e), where we compare this angle-integrated EDC with the EDC at the

antinodal k_F acquired with a resolution of 17 meV. The sharp spectral peaks we observe near (π, 0) are very different from the broad EDCs reported in most ARPES studies of LSCO.

To determine the superconducting gap, we "symmetrize" the EDCs at k_F to effectively eliminate the Fermi function from the measured ARPES spectra [7]. At the antinode, the symmetrized EDC shows two sharp peaks with a clearly defined gap, EDC 7 in Fig. 3(a). Moving from the antinode towards the node along the underlying
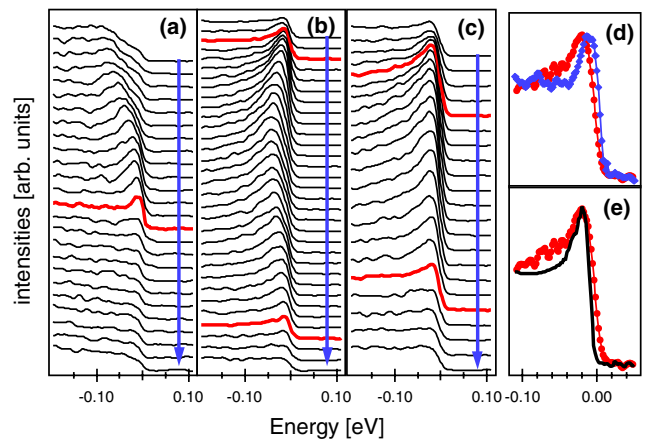

FIG. 2 (color online).   (a)–(c) EDCs along the momentum cuts 1, 3, and 7 in Fig. 1(h). The corresponding momentum ranges are indicated in Figs. 1(a), 1(c), and 1(g) with arrows. Thick curves are EDCs at k_F. (d) Comparison of the EDCs at the antinode (left curve) and at the node (right curve). (e) Comparison of the EDC at the antinode with $h\nu = 55$ eV and an energy resolution of 17 meV (solid symbols), and the angle-integrated EDC over the momentum range marked by the arrow in Fig. 1(g) acquired with $h\nu = 25$ eV an energy resolution of 12 meV (solid line).
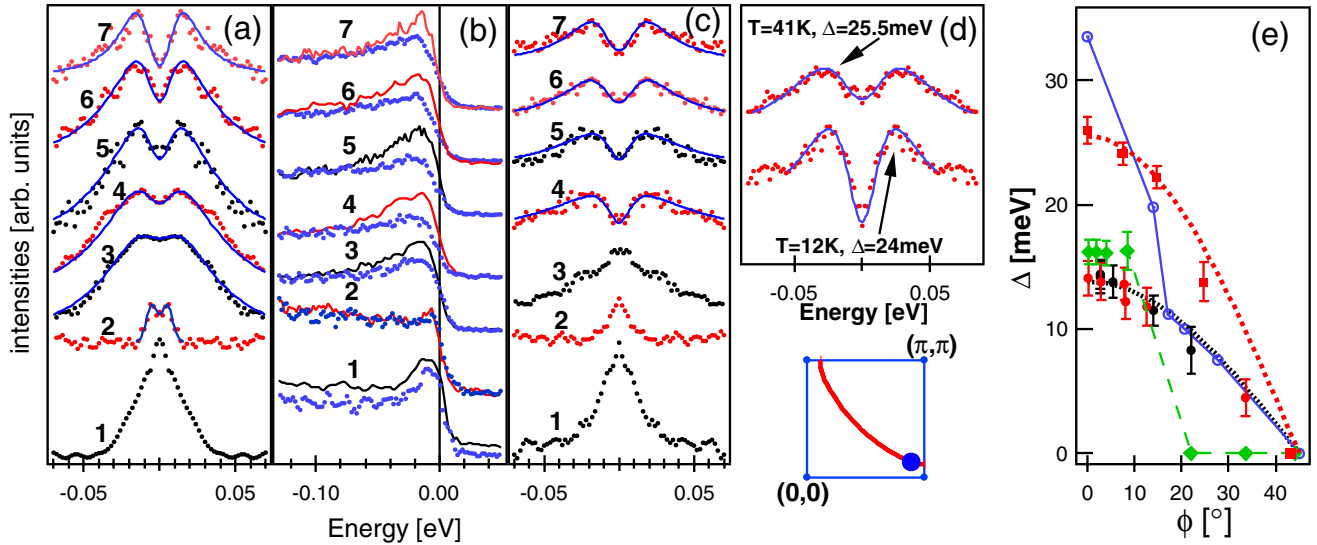
FIG. 3 (color online).   (a) and (c) Symmetrized EDCs for $x = 0.145$ at various k_F from the antinode (top) to the node (bottom) (each curve is offset for clarity) at 12 and 41 K, respectively. The corresponding k_F from cuts 1–7 are indicated in Fig. 1(h) by solid circles. The k_F for cuts 1, 3, and 5 are on the upper underlying FS curve, and the rest are on the lower underlying FS curve. The solid lines are fits using Eqs. (1) and (2). (b) The EDCs at 12 K (solid lines) and at 41 K (dotted lines) from which the symmetrized EDCs in (a) and (c) are obtained. (d) Symmetrized EDCs for $x = 0.105$ at the k_F shown below the panel. (e) The superconducting gaps for $x = 0.105$ (solid squares), the superconducting gaps (solid circles) and the pseudogaps for $x = 0.145$ (diamonds connected with a dashed line) from the fit as a function of the underlying FS angle ϕ indicated in Fig. 1(h), with the dotted lines the simple d-wave gap $\Delta_{max}|\cos(2\phi)|$ with $\Delta_{max} = 13.8$ and 25.5 meV, respectively. The open circles are the gaps determined by Terashima *et al.* for a LSCO sample with $x = 0.15$ [10]. The data were acquired with $h_\nu = 55$ eV.

FS, the separation between the two peaks becomes smaller, and the spectral weight at zero energy fills in, but a two-peak structure is always evident, even for EDC 3 where the gap and spectral width are comparable. Closer to the node, the spectral gap continues to decrease, and finally, when the node is reached, a single peak in the symmetrized EDC is seen (EDC 1).

To perform a more quantitative analysis of the super-conducting gap, we use a simple form for the self-energy that has proven successful in modeling ARPES data [16]

$$\Sigma(k_F, \omega) = -i\Gamma_1 + \frac{\Delta^2}{\omega + i\Gamma_0}, \qquad (1)$$

which is then used to calculate the spectral function

$$A(k_F, \omega) = \frac{1}{\pi} \frac{\text{Im}\Sigma}{(\omega - \text{Re}\Sigma)^2 + (\text{Im}\Sigma)^2}. \qquad (2)$$

This is then convolved with the experimental resolution and fitted to the symmetrized EDC. Here Γ_1 is the single-particle scattering rate, and Γ_0 is related to the inverse pair lifetime. The fitted curves are plotted as solid lines in Fig. 3(a). The best fit was achieved at the antinode where the separation of the two peaks is the largest, with $\Delta = 13.8 \pm 1.5$ meV, $\Gamma_1 = 38 \pm 3$ meV, and Γ_0 is negligibly small (less than 0.1 meV). Near the node, we find $\Gamma_1 \sim 9$ meV, a scattering rate that compares well with the one estimated from the recent infrared conductivity measurements on $La_{1.83}Sr_{0.17}CuO_4$ in Ref. [17]. The negligibly

small value of Γ_0 indicates that the gap at the antinode is associated with pairs which have infinite lifetime (long range order) in the superconducting state. Moreover, the variation of the amplitude of the gap follows a simple d-wave form over the entire FS, Fig. 3(e).

We now address the issue about the existence of the pseudogap above T_c in LSCO ($x = 0.145$) samples. In Fig. 3(b) we plot the EDCs taken at 41 K along the under-lying FS and compare them with those taken at 12 K. While at the node the EDC at 41 K is still characterized by a sharp spectral peak, the EDCs for the antinodal region are characterized by broad peaks with a suppression of spectral weight relative to those below T_c. The symme-trized EDCs [Fig. 3(c)] clearly show that above T_c there is a gap in the electronic excitation spectra in the antinodal region and there is a Fermi arc along which the excitation spectra are gapless. The maximal size of the pseudogap as extracted from the fits by using Eqs. (1) and (2) has a similar amplitude to that of the superconducting gap [Fig. 3(e)]. It should be noted that the determined pseudo-gap is much smaller than that reported in Refs. [10,18].

Our ARPES results on LSCO for $x = 0.145$ are consis-tent with one gap in the superconducting state, but not with a gap having two components, namely, a superconducting gap along the Fermi arc and a pseudogap in the antinodal region with a higher energy scale as seen in previous photoemission studies of LSCO [10,18], as well as under-doped Bi2212 [12] and optimally doped Bi2201 [11]. The first difference is that we observe sharp spectral peaks

along the entire underlying FS, while spectra in these other studies are broad in the antinodal region. The second difference concerns the momentum dependence of the energy gap. In the arc region, the gaps from all of these studies follow a simple *d*-wave form. But in the antinodal region, the gaps in the other ARPES studies cross over to a abnormally large pseudogap at the same location where the sharp spectral peak disappears. But in our case, the sharp spectral peak remains and the gap continues to follow the simple *d*-wave form, with a maximum value of 14 meV at the antinode.

The one-gap nature of underdoped cuprates is further supported by our ARPES results on more underdoped LSCO ($x = 0.105$) which, as for the $x = 0.145$ samples, reveal (1) the symmetrized EDCs near the antinode below (above) T_c are characterized by sharp (broad) peaks [Fig. 3(d)], (2) the maximal gap in the electronic excitation spectra below and above T_c has a similar amplitude, and (3) the anisotropy of the energy gap in the superconducting state is consistent with a *d*-wave form [Fig. 3(e)], though more data will be needed near the node in order to determine whether any gap flattening is present as observed in underdoped Bi2212 [19]. In addition, we find that the maximal gap for $x = 0.105$ is almost twice that of $x = 0.145$. This increase in the energy gap with underdoping follows the same trend as previously observed in Bi2212 [3,4,19].

From the momentum dependence of the gap and the observation that this gap is always associated with a sharp spectral peak, we conclude that the gap we measured below T_c is associated with the *d*-wave superconducting order parameter. Several scenarios can be put forward to explain the difference between our data and those reported earlier. One possibility may be due to increased scattering in the antinodal region resulting from disorder or imperfection that, depending on the sample quality, varies in magnitude. The fact that the samples used for our study appear to be of superior quality is confirmed by two neutron scattering experiments performed on the same sample [20], where (1) a clear vortex lattice could be measured, and (2) a clean spin gap could be observed below T_c, which, in LSCO, is known to be visible only in high-quality samples. Several factors can affect the quality of the samples and, consequently of the ARPES spectra. Of crucial importance is the sample preparation, but other factors such as how the samples are cleaved can play an important role. We have noticed that the specially designed cleaver mentioned above [15] enables us to obtain data of higher quality than that obtained using the very popular "post and glue" cleaving method. Finally, it is interesting to notice that the weak (strong) sensitivity of the nodal (antinodal) states to disorder is consistent with scanning tunneling spectroscopy (STM) studies of Bi2212 [21]. In these STM studies, spectra for biases comparable to that of the antinodal states showed strong sensitivity to spatial location, accompanied by a large distribution of gap sizes. For low biases, though, with energies comparable to states near the node, the spectra are homogenous.

In summary, we have measured the superconducting gap and its momentum dependence by ARPES in moderately underdoped LSCO at temperatures well below T_c. For $x = 0.145$ the anisotropy of the gap follows a simple *d*-wave form, similar to that observed in optimally and overdoped Bi2212. We find no evidence for the coexistence of a superconducting gap and a pseudogap, and relate this finding to the presence of sharp spectral peaks along the entire underlying FS. Such sharp features at the nodal and antinodal points remain even at the lower doping level of $x = 0.105$, although more data closer to the nodal point will be needed in order to determine the precise momentum dependence of the *d*-wave gap in this case. Whether our one-gap scenario continues to hold for more underdoped LSCO samples will be an important matter for future studies.

[1] J. Bardeen, L. N. Cooper, and J. R. Schrieffer, Phys. Rev. **108**, 1175 (1957).

[2] J. G. Bednorz and K. A. Müller, Z. Phys. B **64**, 189 (1986).

[3] J. C. Campuzano, M. R. Norman, and M. Randeria, in *Physics of Superconductors*, edited by K. H. Bennemann and J. B. Ketterson (Springer, Berlin, 2004), Vol. II, p. 167.

[4] A. Damascelli, Z.-X. Shen, and Z. Hussain, Rev. Mod. Phys. **75**, 473 (2003).

[5] H. Ding *et al.*, Nature (London) **382**, 51 (1996).

[6] A. G. Loeser *et al.*, Science **273**, 325 (1996).

[7] M. R. Norman *et al.*, Nature (London) **392**, 157 (1998).

[8] M. R. Norman, D. Pines, and C. Kallin, Adv. Phys. **54**, 715 (2005).

[9] M. Hashimoto *et al.*, Phys. Rev. B **75**, 140503(R) (2007).

[10] K. Terashima *et al.*, Phys. Rev. Lett. **99**, 017003 (2007).

[11] T. Kondo *et al.*, Phys. Rev. Lett. **98**, 267004 (2007).

[12] K. Tanaka *et al.*, Science **314**, 1910 (2006).

[13] A. Kanigel *et al.*, Phys. Rev. Lett. **99**, 157001 (2007).

[14] T. Nakano *et al.*, J. Phys. Soc. Jpn. **67**, 2622 (1998).

[15] M. Månsson *et al.*, Rev. Sci. Instrum. **78**, 076103 (2007).

[16] M. R. Norman *et al.*, Phys. Rev. B **57**, R11093 (1998).

[17] J. Hwang *et al.*, Phys. Rev. Lett. **100**, 137005 (2008).

[18] T. Yoshida *et al.*, J. Phys. Condens. Matter **19**, 125209 (2007).

[19] J. Mesot *et al.*, Phys. Rev. Lett. **83**, 840 (1999).

[20] J. Chang *et al.*, Phys. Rev. Lett. **98**, 077004 (2007).

[21] K. McElroy *et al.*, Phys. Rev. Lett. **94**, 197005 (2005).